A Tonian age of the Visingsö Group in Sweden constrained by detrital zircon dating and biochronology: implications for evolutionary events

MAŁGORZATA MOCZYDŁOWSKA[1], VICTORIA PEASE[2], SEBASTIAN WILLMAN[1], LINDA WICKSTRÖM[3], AND HEDA AGIĆ[1]

[1]Uppsala University, Department of Earth Sciences, Palaeobiology, Villavägen 16, SE 752 36 Uppsala, Sweden, malgo.vidal@pal.uu.se.
[2] Stockholm University, Department of Geological Sciences, PetroTectonics Facility, Svante Arrhenius väg 8, SE 106 91 Stockholm, Sweden.
[3]Geological Survey of Sweden, Box 670, SE 751 28, Uppsala, Sweden.

Author for correspondence: Małgorzata Moczydłowska, Uppsala University, Department of Earth Sciences, Palaeobiology, Villavägen 16, SE 752 36 Uppsala, Sweden. Tel.: +46 184712743; e-mail: malgo.vidal@pal.uu.se.

Abstract – Detrital zircon U-Pb ages from samples of the Neoproterozoic Visingsö Group, Sweden, yield a maximum depositional age of ≤886±9 Ma (2σ). A minimum depositional age is established biochronologically using organic-walled and vase-shaped microfossils present in the upper formation of the Visingsö Group; the upper formation correlates with the Kwagunt Formation of the 780–740 Ma Chuar Group in Arizona, USA, and the lower Mount Harper Group, Yukon, Canada that is older than 740 Ma. Mineralized scale microfossils of the type recorded from the upper Fifteenmile Group, Yukon, Canada, where they occur in a narrow stratigraphic range and are younger than 788 Ma, are recognized for the first time outside Laurentia. The mineralized scale microfossils in the upper formation of the Visingsö Group seem to have a wider stratigraphic range, and are older than c. 740 Ma. The inferred age range of mineralized scale microfossils is 788–740 Ma. This time interval coincides with the VSM range because both microfossil groups co-occur. The combined isotopic and biochronologic ages constrain the Visingsö Group to between ≤886 and 740 Ma, thus Tonian in age. This is the first robust age determination for the Visingsö Group, which preserves a rich microfossil assemblage of worldwide distribution. The organic and mineralized

microorganisms preserved in the Visingsö Group and coeval successions elsewhere document global evolutionary events of auto- and heterotrophic protist radiations that are crucial to reconstruction of eukaryotic phylogeny based on the fossil record and are useful for the Neoproterozoic chronostratigraphic subdivision.

Keywords: Tonian Visingsö Group, detrital zircon, microfossils, eukaryotic evolution, Baltica

1. Introduction

The tripartite subdivision of the Neoproterozoic Era (ICS Timescale, 2015) reflects the time intervals characterized by global environmental changes related to plate tectonics, climate fluctuations, ocean geochemistry and redox state (Johnston *et al*. 2010; Van Kranendonk *et al*. 2012; Lyons, Reinhard & Planavsky, 2014; Planavsky *et al*. 2015). The natural environments shaped the ecosystems and stimulated evolutionary modifications of the highest amplitudes in marine realm. The divergence of eukaryotic protists and finally multicellular organisms including animals (Narbonne, 2005; Knoll *et al*. 2006; Porter, 2006; Butterfield, 2011; Knoll, 2014) might have been triggered, along with genetic mutations, by the development of progressively oxygenated marine basins, which existed in warm to temperate climatic zones (Li, Evens & Halverson, 2013; Spence, Le Heron & Fairchild, 2016; Turner & Bekker, 2016). The oxygenation of marine basins could have also been influenced by the evolution of increasingly complex eukaryotes (Lenton *et al*. 2014) but also the eukaryotes evolution been more independent of oxygen concentration (Butterfield, 2009; Sperling *et al*. 2013; Milles *et al*. 2011). The oxygen level rose due to the steady-state photosynthetic production of free oxygen (Condon *et al*. 2015; Jackson, 2015; Schirrmeister, Gugger & Donoghue, 2015), and cyanobacteria and red and green algae thrived at the time (Schopf, 1992; Butterfield, 2000; Sergeev, 2006; Moczydłowska, 2008a, 2015; Love *et al*. 2009; Moczydłowska *et al*. 2011;

Tang *et al*. 2013; Xiao *et al*. 2014a, b). Oxygen started to accumulate in the atmosphere-hydrosphere system after the Great Oxydation Event (c. 2.3 Ga; Holland, 2002; Bekker *et al*. 2004) or possibly earlier (Lyon, Reinhard & Planavsky, 2014; Jackson, 2015; Lalonde & Konhauser, 2015). The ocean redox state fluctuated but oxygen content increased in the Neoproterozoic (Halverson *et al*. 2010; Planavsky *et al*. 2015; Sahoo *et al*. 2016). Although low atmospheric oxygen concentrations might have prevailed during the mid-Proterozoic (Lyons, Reinhard & Planavsky, 2014; Planavsky *et al*. 2014; Li *et al*. 2015), oxygen concentrations might have been higher (Cox *et al*. 2016; Mukherjee & Large, 2016; Tang *et al*. 2016; Zhang *et al*. 2016), including a ventilated or relatively well-oxygenated surface ocean with oxygen oases or oxygen whiffs (Anbar *et al*. 2007; Kaufman, Corsetti & Varni, 2007; Poulton & Canfield, 2011; Partin *et al*. 2013) possibly allowing the deep ocean to remain anoxic and sulphidic (Canfield, 1998; Anbar & Knoll, 2002).

During the Tonian Period (1000–720 Ma), the supercontinent Rodinia was fragmented and rifted along newly formed continental margins creating seaways with active circulation, mixing water masses and increased input of mineral nutrients from weathering of continental crust (Halverson *et al.* 2010; Li, Evens & Halverson, 2013; Spence, Le Heron & Fairchild, 2016). The subsequent collapse of many ecosystems during the Cryogenian Period (720–635 Ma) due to severe ice ages (Hoffman & Schrag, 2002; Eyles & Januszczak, 2007; Allen & Etienne, 2008; Arnaud, Halverson & Shields-Zhou, 2011), caused the extinction of the majority of biotas (Knoll, 1994; Vidal, 1994; Vidal & Moczydłowska-Vidal, 1997). However, this extinction process or reduction in diversity might have been initiated before the onset of the Sturtian glaciation, thus in the late Tonian, due to eutrophication (Nagy *et al*. 2009) or other as yet unclear factors (Riedman *et al*. 2014). Despite the catastrophic Cryogenian environmental conditions, some lineages and discrete cyanobacterial and algal taxa survived the ice ages and even meantime originated (*Papillomembrana*), as well as ciliates and

foraminifera, during the interglacial cycle(s), as evident from the fossil record in the pre-, inter-, and post-Cryogenian successions (Corsetti, Awramik & Pierce, 2003; Moczydłowska 2008a, 2008b; Nagy *et al*. 2009; Bosak *et al*. 2011, 2012; Riedman *et al*. 2014; Cohen *et al*. 2015; Corsetti, 2015; Ye *et al*. 2015). The recovery of ecosystems following de-glaciation and sea-level rise in the Ediacaran Period (635–541 Ma) paved the way for the exponential radiation of phytoplankton, the rise of multicellular organisms of the Ediacara-type, and the bilaterian animals of modern phyla (Grey, 2005, 2007; Narbonne, 2005; Moczydłowska & Nagovitsin, 2012; Narbonne, Xiao & Shields, 2012; Liu *et al*. 2014; Xiao *et al*. 2014a).

The environmental and evolutionary history of the Tonian Period is renowned for the development of marine habitats that sustained robust planktic and benthic communities, and induced further life expansion as is shown by the high diversification of auto- and heterotrophic protists (Vidal & Moczydłowska-Vidal, 1997; Knoll *et al*. 2006; Porter, 2006; Sergeev, 2006; Cohen & Knoll, 2012; Cohen & Macdonald, 2015). However, several microfossil taxa (*Pterospermopsimorpha, Valeria, Tasmanites*, *Schizofusa*; certain *Leiosphaeridia*) have persisted since the Mesoproterozoic Era (Yan & Liu, 1993; Lamb *et al*. 2009; Moczydłowska *et al*. 2011; Agić, Moczydłowska & Yin, 2015a). The Tonian diversification is well recorded in the Visingsö Group of the Lake Vättern Basin (Fig. 1) and in numerous successions worldwide, such as the Vadsø, Tanafjord and Hedmark groups in Norway, successions in Russia (the southern Urals and Siberia), the USA (the Chuar Group in Arizona, Uinta Mount Group in Utah, and the Pahrump Group in California), Canada (the Fifteenmile and Harper groups in Yukon), and in China (the Gouhou Formation) (Vidal, 1976; Vidal & Ford, 1985; Jankauskas *et al*. 1989; Horodyski, 1993; Vidal & Moczydłowska, 1995; Porter, 2006; Nagy *et al*., 2009; Cohen & Knoll, 2012; Strauss *et al*. 2014; Tang *et al*. 2015; Porter & Riedman, 2016). The Visingsö Group contains a diverse assemblage of cyanobacteria, stromatolites, organic-walled microfossils (OWM), and vase-shaped

111 microfossils (VSM) (Vidal, 1972, 1976; Martí Mus & Moczydłowska, 2000; Agić,
112 Moczydłowska & Willman, 2015b; Loron, 2016). In addition, newly recovered mineralized
113 scale microfossils (MSM; Fig. 2a, b, d; ongoing study) resemble the type known from the
114 Tonian Fifteenmile Group in Yukon, Canada (former Tindir Group; Allison & Hilgert, 1986;
115 Macdonald *et al*. 2011; Cohen & Knoll, 2012).

116 Until now, the age of the Visingsö Group was estimated palaeontologically to between
117 800–700 Ma (Vidal & Moczydłowska, 1995). Our dating of detrital zircons provides a
118 maximum depositional age of c. 886 Ma and, together with the biochronology of common
119 microfossil taxa established in the Chuar and Mount Harper groups at minimum age of c. 740
120 Ma (Dehler *et al*. 2005; Nagy *et al*. 2009; Strauss *et al*. 2014), is consistent with a Tonian age
121 of the Visingsö Group.

122 The implications of the Visingsö microfossil record set within a geochronologic
123 framework are significant for reconstructing Neoproterozoic evolutionary events and
124 ecological processes. These are the origin and divergence of phytoplanktic (many OWM) and
125 heterotrophic (VSM) protists, MSM of uncertain but likely algal affinity (Cohen *et al*. 2011),
126 and benthic bacteria forming microbial mats and stromatolites. Their passive dispersal (cysts
127 of algal phytoplankton and heterotrophs) or active migration (motile vegetative cells of
128 phytoplankton and motile heterotrophic protists) in the marine realm were facilitated by the
129 global hydrological cycle and patterns of current circulation changing at given time intervals
130 throughout the Neoproterozoic.

131

132 **2. Geological setting**

133 The Mesoproterozoic Sveconorwegian belt exposed in southwestern Scandinavia (Fig.
134 1A) represents deeply eroded continental crust reworked during Sveconorwegian (1.14–0.90
135 Ga) orogenesis (Möller *et al*. 2015 and references therein). The later is associated with the

136 construction of Rodinia (Pease *et al*. 2008; Bingen, Belousova & Griffin, 2011). Post-
137 orogenic relaxation and gravitational collapse led to uplift and cooling at c. 900 Ma (Viola *et*
138 *al.* 2011). Scandinavia, as part of Baltica, gradually rifted from Rodinia between c. 850–630
139 Ma with concomitant marine transgression (Li, Evens & Halverson, 2013). This paper focuses
140 on the Tonian (1000–720 Ma) depositional history of Fennoscandia.

141 During Sveconorwegian orogenesis, southeastward imbrication and displacement of
142 the crust occurred. The eastern limit of the orogen is defined by the Sveconorwegian
143 deformation front (SF), a steeply dipping zone of high strain that marks the limit of
144 Sveconorwegian ductile deformation and metamorphism (Möller *et al*. 2015; Fig. 1a). To the
145 east of the SF, igneous and metamorphic rocks of the 2.0–1.75 Ga Svecokarelian orogen and
146 1.86–1.66 Ga plutonic and volcanic rocks of the Transcandinavian Igneous Belt (TIB) are
147 unaffected by Sveconorwegian ductile deformation or metamorphism (Stephens *et al*. 2009).
148 The orogen-parallel 0.97–0.95 Ga Blekinge-Dalarna dolerite dike swarm intrudes along and
149 east of the SF (Söderlund *et al*. 2005) and documents the last known magmatic activity along
150 the SF. The SF is a long-lived crustal-scale feature. It was active as early as c. 1200 Ma
151 during the early phase of Sveconorwegian orogenesis, and was reactivated later (c. 950 Ma)
152 during uplift of the Eastern Segment (e.g. Viola *et al*. 2011). This was followed by the
153 formation of the "proto-Vättern graben" with deposition of the Visingsö Group in the
154 Neoproterozoic (Vidal & Moczydłowska, 1995).

155 Late to post-Sveconorwegian sediments are not preserved within the Sveconorwegian
156 belt. Post-orogenic sediments interpreted to reflect rift- and passive-margin settings associated
157 with the break-up of Rodinia were deposited in the Sveconorwegian hinterland (Pease *et al*.
158 2008). These are now preserved within the nappes (Hedmark Group) and parautochthonous
159 successions (Vadsø and Tanafjord groups) of the Caledonian orogen (Bingen, Belousova &
160 Griffin, 2011). Along the SF, erosional remnants of these sediments, e.g. the Visingsö Group,

the Amesåkra Group, the Dala Sandstone and successions in the Sparagmite Basin, unconformably overlie TIB granitoid basement (Bingen et al., 2011; Lundmark & Lamminen, 2016; Fig. 1a, b).

3. Visingsö Group succession, previous work and sampling

The Visingsö Group is exposed along Lake Vättern and on Visingsö Island. The Group consists of terrigeneous clastic rocks with minor carbonates deposited on TIB-related rocks of various ages (Vidal, 1974, 1976, 1982, 1985; Larson & Nørgaard-Pedersen, 1988; Ulmius, Andersson & Möller, 2015; Fig. 1b). The succession is also known from 15 boreholes penetrating various portions of the strata. The Visingsö strata are unmetamorphosed and undeformed except for local normal faults with low dips of 5–25° (Vidal, 1976; Morad & Al-Aasm, 1994). The Visingsö Group is about 1426 m thick and comprises a lower, middle and upper formation (informal nomenclature; Fig. 1c). The lower formation consists of quartzofeldspathic sandstone interbedded with shale and arkosic sandstone (over 400 m in thickness), and represents a progradational fluvial-deltaic environment. The boundary between the lower and middle formation is gradational from quartzitic sandstone coarsening into feldspathic sandstone, respectively. The middle formation comprises feldspathic sandstone and conglomerate succeeded by alternating sandstone, mudstone and shale (at least 446 m), deposited in a pro-delta setting characterized by occasional delta lobes prograding into shallow marine environments. The boundary with the upper formation is sharp at the top of quartz sandstone (middle formation) and the base of laminated mudstone (upper formation). The upper formation consists of alternating shale, mudstone and fine-grained sandstone, and dolomitic limestone with stromatolites (580 m thick). Deposition occurred in a shallow marine tidally-influenced mud flat environment with distinct intervals of subtidal and intertidal sedimentation.

Geological relationships indicate that the Visingsö Group sediments are younger than c. 946 Ma, the age of dolerite dikes that cut the granitoid basement upon which the Group is deposited (Söderlund *et al*. 2005). Earlier isotopic studies of the Visingsö Group include K-Ar detrital mica ages (1060–985 Ma; Magnusson, 1960) and Rb-Sr ages on clay and whole rock fractions of shale from the upper formation (703–663 Ma; Bonhomme & Welin, 1983) – ages now interpreted to reflect the time of crystallization and diagenesis, respectively.

We examine three samples from the Visingsö Group at Lake Vättern (Fig. 1b). The lower formation sample (V15-Lem) was collected from the NE wall at the entrance to the Lemunda Quarry, and consists of white-yellowish, medium-grained, weakly consolidated quartz arenite with faint thin bedding. Two samples of the middle formation were collected from the Visingsö 1 borehole on Visingsö Island (Fig. 1b) at depths of 137.50–140.10 m (V15-10) and 120.40–120.95 m (V15-9). They are medium-grained quartzofeldspathic sandstone.

4. Age and provenance of the Visingsö Group from detrital zircon

4.a. Analytical methods

Zircons were separated from 1–2 kg of sample using conventional water table and heavy liquid mineral separation techniques. Approximately 200 zircon grains with various morphologies, sizes and colors were hand-picked onto double-sided tape, cast into epoxy resin, sectioned and polished. A deliberate effort was made to select all zircon colors, sizes, morphologies, etc., during picking. Scanning electron microscope (SEM) and cathodoluminescence (CL) images of zircon were used to identify textures and select analytical locations; these were obtained using a FEI SEM at the Department of Geological Sciences, Stockholm University. Analytical methods follow those described in Zhang, Roberts & Pease (2015a). Further details of the analytical method are provided in Appendix 1.

4.b. Analytical results

Our analytical results are summarized below and in Fig. 4. The data and inverse concordia diagrams, as well as a more detailed discussion of sediment provenance, are also presented in Appendix 1 (Table A2, and figures A1, A2, and A3). Errors are reported at the 2-sigma level. For zircon ages younger than 1.2 Ga the 206Pb/238U ages were used in the final analysis and for ages older than 1.2 Ga the 207Pb/206Pb ages were used in the final analysis. Analyses with high common Pb as well as those with >10% discordance or >10% uncertainties, were excluded from the final data synthesis. Concordia diagrams and probability density distribution plots were made using ISOPLOT/Ex 4.15 (Ludwig, 2008).

V15-Lemunda. The lower formation of the Visingsö Group. Zircon from this quartz arenite reflects a diverse detrital assemblage of grains, i.e.- aspect ratios of 1:1 to 1:5, a variety of colors, with and without inclusions, a range of cathodoluminesence (CL) textures from igneous oscillatory zoning to uniformly bleached zones indicating secondary fluid migration. The grains are generally low in U (500 ppm or lower in 93% of the crystals) with diverse Th/U ratios (0.14-2.1). Seventy percent of the analyses meet the quality assessment criteria (117/154), yielding a continuous spread of ages from 1850-887 Ma (Appendix 1, Fig. A1). Neoproterozoic peaks at c. 1026, 945, and 900 Ma dominate the age spectra, while lesser peaks occur at c. 1600, 1446, 1268 and 1100 Ma (peak ages typically ± 25 Ma). A weighted mean of the youngest four analyses = 886 ± 9 Ma (MSWD = 0.81, Prob = 0.49) and provides a conservative maximum age of the sediment.

V15-10. The middle formation of the Visingsö Group. Zircon from this quartz-arkosic sandstone, similar to V15-Lem, reflects a diverse detrital assemblage of grains with the addition of CL-dark rim overgrowths on most grains. The grains have moderate U concentrations with 77% between 100-700 ppm, 13% <100 ppm, and 10% >1000 ppm. Modern lead-loss is apparent in the 238U/206Pb versus 207Pb/206Pb concordia diagram, in

accord with high-U grains and metamictization. Th/U ratios are diverse (0.08-2.4). Sixty percent of the analyses meet the quality assessment criteria (98/165), yielding a continuous spread of ages from 1913-990 Ma (Appendix 1, Fig. A2). Paleoproterozoic to Mesoproterozoic peaks dominate the age spectra, namely c. 1751, 1625, and 1450 Ma, while a spread of ages occurs at c. 1300-990 Ma with a minor peak at c. 992 Ma. A weighted mean of the youngest three analyses = 997 ± 13 Ma (MSWD = 0.38, Prob = 0.68) and provides the maximum age of the sediment.

V15-9. The middle formation of the Visingsö Group. Zircon from this quartz-arkosic sandstone also reflects a diverse detrital assemblage of grains with the addition of CL-dark rim overgrowths on most grains. The grains range from 32-1152 ppm U, with 71% between 100-500 ppm, and 5% >1000 ppm. Modern lead-loss is also apparent in the 238U/206Pb versus 207Pb/206Pb concordia diagram. Th/U ratios are diverse (0.04-3.6). Seventy-five percent of the analyses meet the quality assessment criteria (132/168) and yield a continuous spread of ages from 1878-1043 Ma (Fig. A3). The dominate peaks in the detrital spectra are Mesoproterozoic in age, namely c. 1640, 1580, and 1439 Ma, while older (c. 1780 Ma) and younger ages (c. 1260-1045 Ma) are minor contributors to the age spectra. A weighted mean of the two youngest analyses = 1050 ± 15 Ma (MSWD = 0.57, Prob = 0.45) and provides a maximum age for the sediment.

Our new LA-ICP-MS U-Pb detrital zircon data from the three Visingsö samples provide maximum depositional ages for the middle formation of ≤1050±15 Ma (2σ; V15-9) and ≤997±13 Ma (2σ; V15-10), and for the lower formation of ≤886± 9 Ma (2σ; V15-Lem) (Fig. 4). The youngest age, obtained from the lower formation, represents the best estimate of the maximum depositional age for the Visingsö Group at c. 886 Ma.

4.c. Provenance

261 The provenance of the Visingsö zircons is consistent with derivation from the igneous,
262 metamorphic and recycled sedimentary rocks known to be exposed in the region at the time of
263 deposition, i.e.- Svecokarelian rocks (c. 2.0–1.75 Ga), TIB (c. 1.86–1.66 Ga plutonic and
264 volcanic rocks), metamorphic and igneous rocks associated with the Gothian (1.66–1.52 Ga),
265 Hallandian (c. 1.47–1.38 Ga), and Sveconorwegian (c. 1.14–0.90 Ga) orogens (Lundmark and
266 Lamminen, 2016; Möller et al., 2015), as well as swarms of 1.6–0.95 Ga dolerite dikes
267 (Söderlund et al., 2005) that intrude the Fennoscandian basement. In addition, the Meso- to
268 Neoproterozoic sediments now only locally preserved across the shield (e.g., Morad and Al-
269 Aasm, 1994; Bingen et al., 2011; Lundmark and Lamminen, 2016; Fig. 1a), sources within
270 the Sveconorwegian belt that include a far-traveled Laurentian component, and sources from
271 Fennoscandia east of the belt (Bingen et al., 2011) are also potential contributors. Thus, we
272 regard the Visingsö Group as predominantly regionally derived.
273

274 **5. Age of the Visingsö Group from diagnostic assemblages**

275 An approximate relative age of c. 800–700 Ma for the Visingsö Group has been previously
276 inferred by correlating diagnostic assemblages of OWM, VSM and stromatolites with
277 successions that have an established chronostratigraphy (Vidal & Moczydłowska, 1995; Martí
278 Mus & Moczydłowska, 2000). Such assemblages are known from the Hedmark, Vadsø and
279 Tanafjord groups in the Caledonides of Norway, the Thule and Eleonore Bay groups of
280 Greenland, the Chuar, Uinta Mountain, and Pahrump groups in the western USA, the Little
281 Dal, Mount Harper and Fifteenmile groups in Canada, and others in Siberia, the Urals, and
282 Svalbard (Vidal, 1976; Vidal & Ford, 1985; Horodyski, 1993; Vidal & Moczydłowska-Vidal,
283 1997; Porter & Knoll, 2000; Porter, 2006; Nagy *et al*. 2009; Strauss *et al.* 2014). Recent
284 datings of the successions in the western USA and Canada provide more accurate age
285 constraints (Strauss *et al*. 2014). The VSM and certain OWM taxa in the upper formation of

286 the Visingsö Group (Figs. 2–3; Appendix 2, List of species), which co-occur in the Kwagunt
287 Formation (the upper Chuar Group), and the Callison Lake dolostone (the lower Mount
288 Harper Group), provide a biochronological minimum age for the Visingsö Group of c. 740
289 Ma (see discussion below). Thus the Visingsö Group is now robustly constrained to <886–
290 740 Ma.
291
292 **6. Discussion and evolutionary implications**
293 The Tonian Visingsö Group documents a diverse microbial association of prokaryotic
294 cyanobacteria and eukaryotic OWM, VSM (Vidal, 1972, 1976; Martí Mus & Moczydłowska,
295 2000; Agić, Moczydłowska & Willman, 2015b; Loron, 2016), and new MSM that are partly
296 identified. The MSM could represent biomineralizing green algae (Cohen *et al*. 2011; Cohen
297 & Knoll, 2012) adding another dimension to the complex ecosystem and development of
298 biomineralization. A new record of OWM, including *Cerebrosphaera, Valeria, Schizofusa,*
299 *Simia, Tasmanites* and *Pterospermopsimorpha* among other taxa (Fig. 3; Appendix 2),
300 strengthen the ranges of potential species for Neoproterozoic biostratigraphy. These taxa are
301 recognized as possible members of green algal lineages of Prasinophyceae and
302 Chlorophyceae (Grey, 2005; Lamb *et al*. 2009; Moczydłowska *et al*. 2011; Moczydłowska,
303 2015; Agić, Moczydłowska & Willman, 2015b; Loron, 2016), but many other OWM taxa
304 remain unidentified phylogenetically. Geochronologically better understood, and now
305 constrained by isotopic dating, the Visingsö microbiota will contribute to reconstructing the
306 relationships among early eukaryotes (Knoll, 2014) by further reconciling the fossil record
307 with molecular clock estimates.
308 The recognition and identification of OWM, VSM, and MSM microfossils allows us to
309 make biochronologic correlations with the Chuar, lower Mount Harper and the upper
310 Fifteenmile groups. The Visingsö microfossils, both uni- and multicellular, are well-

311 preserved, abundant and consist of established as well as new species. Some have features
312 that support their various protistan affinities (ongoing study). The OWM in the Visingsö
313 Group were originally described by Vidal (1976) from all formations and additional records
314 derive from the middle and upper formations (Agić, Moczydłowska & Willman, 2015b;
315 Loron, 2016; ongoing study; Fig. 3, Appendix 2). The assemblage consists of 20 species
316 recognized by distinct morphology (surface sculpture, excystment structure, wall perforation)
317 and bodyplan (sphere-in-sphere, internal body). Several new species, including those with
318 spinous ornamentation, await formal description. A great variety of spheroidal specimens
319 displaying a wide range of vesicle size and wall thickness, which are attributed by some
320 authors to different species of *Leiosphaeridia* (*crassa, jacutica, minutissima*, and *tenuissima*),
321 are left under open nomenclature as *Leiosphaeridia* spp. Their quantity is enormous
322 (thousands of specimens), yet they lack objective morphologic features and overlap in
323 dimensions to make identification reliable. The cyanobacterial coccoidal and filamentous
324 microfossils preserved as solitary specimens, colonies and fragmentary bacterial mats are
325 attributed to 7 genera with more numerous species. In total, the OWM record is among the
326 highest diversity recognized in a single Tonian-age stratigraphic unit. This diversity is of the
327 same taxonomic magnitude as in the Chuar Group assemblage accounting for some 32 OWM
328 species (Nagy *et al*., 2009; Porter & Riedman, 2016), and many are in common. Thus we
329 correlate the middle and upper formations of the Visingsö Group with the Chuar Group. The
330 lower formation of the Visingsö Group consists of spheroidal and cyanobacterial species that
331 are not age-diagnostic.
332 The VSM in the upper formation of the Visingsö Group are recorded in un-
333 metamorphosed phosphate nodules embedded in organic-rich mudstone and shale (Knoll &
334 Vidal, 1980; Martí Mus & Moczydłowska, 2000; unpublished data). The phosphate nodules
335 are composed of francolite, a cryptocrystalline phosphate. These were early diagenetically

precipitated in suboxic to sulfate-reduction zones within decimeters to meters of burial below the sediment-water interface (Morad & Al-Aasm, 1994) on tidal mud flats (Larson & Nørgaard-Pedersen, 1988). Francolite precipitation was microbially mediated and microbial mats occur as patches and thin discontinuous laminae in the nodules and host mudstone. VSM are abundant, with up to several hundred specimens present in a single petrographic thin section, and mostly observed in longitudinal or slightly transversal sections. No perpendicular-to-the long axis sections or through the oral part of the tests are seen in thin section.

The VSM preserved as three-dimensional organic-walled tests and extracted by acid maceration are known only from the Eleonore Bay Group of East Greenland (Vidal, 1979), the Kwagunt Formation of the Chuar Group type locality (Bloeser, 1985; Porter & Knoll, 2000; Porter, Meinsterfeld & Knoll, 2003), and from the Tien Shan Mountains in Kyrgyzstan (Jankauskas, Mikhailova & German, 1989). Mostly they are preserved as permineralized casts and molds (Martí Mus & Moczydłowska, 2000; Porter & Knoll, 2000; Porter, Meinsterfeld & Knoll, 2003; Strauss *et al*. 2014). The Visingsö specimens have not yet been isolated from the rock matrix or nodules, and are observed as casts and molds replicated by precipitation of francolite, quartz and berthierine (Martí Mus & Moczydłowska, 2000). Therefore, their identification is limited to the overall habit and symmetry of the tests observed in thin section without oral opening ornamentation and shape. We identified *Melanocyrillium hexadiadema* Bloeser, 1985 (Fig. 2c, upper specimen) by distinguished longitudinal section with test flexure marking the oral termination (neck-like region) and invaginated aperture between broad indentation, though the transversal section of the hexagonal aperture was not seen. Synonymy, based on comparable thin sections of the species, includes specimens illustrated by Bloeser (1985, fig. 7:14; identical to our specimens), Porter, Meinsterfeld & Knoll (2003, fig. 4:11), and Strauss *et al*. (2014, fig. 2A). A specimen with apertural margin with minimal

short collar and flushing into the test wall (Fig. 2b) is similar to a thin section illustration by Porter et al. (2003, fig. 6:21) and attributed to *Cycliocyrillium torquata* Porter, Meisterfeld and Knoll, 2003. The species is also recognized in the assemblage studied by Martí Mus & Moczydłowska (2000; fig. 3A; see Porter, Meinsterfeld & Knoll, 2003), alongside with *Cycliocyrillium simplex* Porter, Meisterfeld and Knoll, 2003 (Martí Mus & Moczydłowska, 2000, fig. 6A, C–F; fig 7A–C, E–F). The latter species is recognized by a bulbous outline of the test with a simple aperture relatively narrow in relation to the test width and without any marginal thickening, as seen in the SEM image and the thin section illustration by Porter, Meinsterfeld & Knoll (2003, fig.6:9). These authors also suggested this species might be present in the Visingsö assemblage studied by Knoll & Vidal (1980, fig. 1D–G), as well as *Trigonocyrillium horodyski* (Bloeser, 1985) Porter, Meinsterfeld and Knoll, 2003, and *T. fibriatum* (Bloeser, 1985) Porter, Meinsterfeld and Knoll, 2003, although the two latter species were without reference to individual specimens or collection. *T. fimbriatum* has been documented only by SEM images in the type collection (Bloeser, 1985) but an elongate test with oral fringe seen in the longitudinal view (Bloeser, 1985, fig. 10:2_1, 4_1, 7_1, and 11:3) is very similar to the specimen illustrated by Martí Mus & Moczydłowska (2000, fig, 2D). This makes a record of five common geographically distributed VSM species in the upper formation of the Visingsö Group among twelve species known in total from the upper Kwagunt Formation (Porter & Knoll, 2000; Porter, Meinsterfeld & Knoll, 2003). Three species (*M. hexadiadema*, *C. simplex*, and *C. torquata*) also co-occur in the assemblage of eight species recorded in the Callison Lake dolostone of the lower Mount Harper Group, Yukon, Canada (Strauss *et al*. 2014). Allison and Awramik (1989) report an older stratigraphic record of VSM in this area (the Tindir Creek, Yukon) from the upper Tindir Group (now the upper Fifteenmile Group; Macdonald *et al*. 2010a, b, 2011; Cohen & Knoll, 2012) that underlies the Callison Lake dolostone and additionally some 670 m thick

succession belonging to the Craggy Dolostone Formation. They document VSM *Melanocyrillium* sp. and new species *Hyalocyrillium clardyi* Allison, 1989, along with MSM. The latter taxon was recognized by Allison and Awramik (1989) as being similar to VSM from the Visingsö Group (and successions in Greenland, Brazil and Saudi Arabia) but different from those in the Chuar Group described by Bloeser (1985) by having a thicker wall. This morphologic or taphonomic difference is insignificant and *H. clardyi* belongs to VSM thus proving the co-occurrence of VSM with MSM (Allison & Awramik, 1989; Cohen & Knoll, 2012).

The new genus and species *Hyalocyrillium clardyi* Allison, 1989 (Allison & Awramik, 1989; fig. 10:10–11) is similar if not identical to *Cycliocyrillium simplex* Porter, Meisterfeld and Knoll, 2003 (Porter, Meinsterfeld & Knoll, 2003, thin section fig. 6:9) and the two taxa are considered conspecific. This synonymy implies that *Hyalocyrillium* Allison, 1989, has taxonomic priority over *Cycliocyrillium* Porter et al., 2003, and its type species *C. simplex* is a junior synonym of the type species *H. clardyi*. Consequently, *C. torquata* Porter et al., 2003 should be transferred to as *H. torquata* (Porter, Meinsterfeld and Knoll, 2003) n. comb.

The range of VSM in Laurentia was recognized within the time interval c. 780–740 Ma (Dehler, 2014; Strauss *et al*. 2014) and, as aforementioned, they extend through a number of formations across the western margin of Laurentia from the Grand Canyon to the Yukon Territory. In the Yukon, the range of VSM through the Callison Lake dolomite (Strauss *et al*. 2014) is in fact wider and extends into the upper Fifteenmile Group to above the isotopically dated layer at 811.5 Ma (Allison & Awramik, 1989; Macdonald *et al*., 2010b; Cohen & Knoll, 2012). This poses the need to i) correlate the upper Fifteenmile Group with other successions containing VSM, and ii) extend the VSM lower range to c. 788 Ma, consistent with the MSM range (see below).

411 MSM occur side-by-side with VSM (Fig. 2b) in the upper formation of the Visingsö
412 Group at two stratigraphic levels (Fig. 1c) and they are of the type of scale-like microfossils
413 known from the 811.5–739.9 Ma Ma upper Fifteenmile Group of the Yukon Territory,
414 Canada (Allison & Hilgert, 1986; Macdonald *et al*., 2010a, b, 2011; Cohen *et al*. 2011; Cohen
415 & Knoll, 2012; Strauss *et al*. 2014). Their discovery in the Visingsö succession for the first
416 time documents their occurrence outside the type locality on Laurentia and is significant
417 because their stratigraphic range is wider than previously recorded. This is evident from their
418 vertical distribution within rock succession of shale and mudstone approximately 300 m thick
419 (Fig. 1c) in comparison to the interval of 58 m of limestone containing MSM in the upper
420 Fifteenmile Group (Cohen & Knoll, 2012). Regardless of different rates of sedimentation
421 between fine-grained siliciclastic vs carbonate rocks in the two localities, and both
422 accumulated in shallow subtidal environments (Larson & Nørgaard-Pedersen, 1988;
423 Macdonald *et al*. 2011, respectively), it appears that the MSM vertical range in the Visingsö
424 Group involves a longer time span.
425 The Visingsö MSM are observed in thin-sections of phosphate nodules in shale and
426 are not yet successfully isolated from the host rock to see their three-dimensional morphology
427 thus making the identification preliminary. They are simple morphotypes, ellipsoidal in
428 outline, smooth in appearance and not perforated, with sharply defined narrow marginal rims
429 and central portion (Figs. 2a, b) or showing additionally one or two marks or holes in the
430 center (Fig. 2d). Their dimensions are 18–39 μm in length, and 1.5–6.0 μm of marginal rim
431 width. The present specimens, by comparison with specimens observed in thin sections of
432 chert nodules but also with those isolated from the Fifteenmile Group limestone, are identified
433 as *Paleomegasquama arctoa* Cohen and Knoll, 2012 (Fig. 2a), *Bicorniculum brochum*
434 Allison and Hilgert, 1986 (Fig. 2b), and *Archeoxybaphon polykeramoides* (Allison and
435 Hilgert, 1986) emend. Cohen and Knoll, 2012 (Fig. 2d). Specimen of *P. arctoa* (Fig. 2a), is an

436 ellipsoidal scale, 21x30 μm in diameter, with smooth surface and two distinct portions:
437 narrow marginal rim 1.5–2.3 μm in width and large central portion. It resembles isolated
438 Fifteenmile specimens of placolith form and is of their dimensions (Cohen & Knoll, 2012, fig.
439 9.7–9.9), and if seen in section it would be identical to the specimen illustrated by Cohen &
440 Knoll (2012, in fig. 9.8). Specimen of *B. brochum* (Fig. 2b) is an ellipsoidal scale, 30x39 μm
441 in diameter, with two marginal rings: narrow inner and wider outer, together 6 μm in width,
442 around central ellipsoidal portion. It is similar to specimens in illustrated thin sections by
443 Allison & Hilgert (1986, figs 10.1 and 10.2), although the tooth-like band is not visible
444 clearly in our section. However, the higher dimensional proportion of the two rings to small
445 central portions of scale is typical of the species and differ from other scale microfossils. The
446 species *A. polykeramoides* is an elliptical scale, 18x25 μm in diameter, smooth without any
447 visible pores, with thin marginal rim and 1-2 central elongate markings or holes. Certain
448 three-dimensionally preserved Fifteenmile Group specimens show elevated elements or holes
449 in central portion of scale (Cohen & Knoll, 2012, figs 3.1 and 3.5), which if sectioned would
450 appear similar to those in the Visingsö specimens (Fig. 2d).
451 The stratigraphic position of MSM in the type area of the Western Ogilvie Mountains,
452 Yukon, in the Lower Tindir Group, upper shale informal unit, has been defined to be above
453 the Bitter Springs C-isotopic anomaly stage which is also recognized in the upper Fifteenmile
454 Group in the Central Ogilvie Mountains above the horizon isotopically dated to 811.5 Ma
455 (Macdonald *et al*. 2010b). The MSM described in detail by Cohen & Knoll (2012) have been
456 subsequently attributed to the upper Fifteenmile Group, and tentatively to its Craggy
457 Dolomite Formation in the Mt. Slipper section, where the fossiliferous strata are 58 m thick.
458 This is the same lithostratigraphic unit as the “limestone unit of the upper Tindir Group” in
459 the Tindir Creek locality studied originally by Allison & Hilgert (1986).
460 Uncertainty remains regarding the lithostratigraphic attribution of MSM, because

461 of recent re-mapping and re-assessment of rock successions in the Yukon Territory, and
462 revision of their stratigraphic position and regional correlation based on isotopic dating and
463 $\delta^{13}C$ chemostratigraphy (Macdonald *et al*. 2010a, b, 2011; Macdonald & Roots, 2010; Strauss
464 *et al*. 2014). The chronostratigraphy of these units is has also changed and previously
465 attributed to the Cryogenian (850–635 Ma) is now referenced to the Tonian Period (1000–720
466 Ma), following the International Chronostratigraphic Chart 2015 (Cohen *et al*. 2015).
467 The stratigraphic position of MSM, whether in the basal Craggy Dolostone or at the
468 top of the Reefal Assemblage, is constrained by the age of the Bitter Springs Stage (BSS).
469 The BSS has been recognized as globally synchronous C-isotope negative anomaly
470 (Halverson *et al*. 2010) and is constrained to the interval after 811.5 Ma and before 788.7 Ma,
471 lasting c. 7–17 Ma (Macdonald *et al*. 2010b; Swanson-Hysell *et al*. 2015). MSM occur above
472 the BSS thus their maximum age is c. 788 Ma. The range of MSM in the Ogilvie Mountains
473 type area is very short and equal to the depositional time of 58 m thick limestone that may be
474 just a few million years calculating from the rate of deposition of the succession (c. 1000 m
475 thick carbonate succession deposited within time interval 811–740 Ma). A wider vertical
476 range and closer to the minimum age of MSM is recorded in the Visingsö Group.
477 MSM in the upper formation of the Visingsö Group co-occur with more diverse VSM
478 taxa known from the upper Kwagunt Formation and the Callison Lake dolostone (including
479 *M. hexadiadema*) and understood to record their upper stratigraphic range and minimum age.
480 This is inferred from the present correlation of the upper formation of the Visingsö Group
481 with these formations and constrained by the minimum age at 740 Ma of the Callison Lake
482 dolostone (Strauss *et al*. 2014). The MSM lower range and maximum age is recognized in the
483 the upper Fifteenmile Group and it coincides also with the earliest occurrence of VSM. The
484 MSM upper range and minimum age is recorded in the upper formation of the Visingsö

485 Group together with those of the VSM and indicate the time span of both microfossil groups
486 at c. 788–740 Ma.

487 Tonian marine ecosystems were dominated, as seen in fossil record by their taxonomic
488 diversity and relative abundance (Porter, 2006; Nagy *et al*. 2009; Cohen & Macdonald, 2015;
489 Tang *et al*. 2015) and enhanced by new record from the Visingsö Group (accounted by
490 thousands specimens; unpublished data), by photosynthesizing cyanobacteria and algae, and
491 less frequently occurring heterotrophic protists, and some protists of uncertain origin
492 (Butterfield, 2000; Porter, 2006; Sergeev, 2006; Cohen & Macfadden 2015; Porter &
493 Riedman, 2016). Shallow marine habitats must have been relatively well oxygenated to
494 sustain planktic and benthic autotrophs, allowing them to fullfill their metabolic and life cycle
495 requirements for sexual reproduction, as known from modern analogues (see discussion by
496 Moczydłowska, 2008a, 2015). Relatively well oxygenated ocean surface waters or at least
497 oxygenated local basins in such state are supported by geochemical studies (Jackson, 2015;
498 Lalonde & Konhauser, 2015; Turner & Bekker, 2016; Spence, Le Heron & Fairchild, 2016)
499 and this is in agreement with the presence of microbiota of inferred algal affinities and
500 sexually reproducing in the Visingsö Group at the time, and in contemporaneous successions.
501 Progressive evolution of phytoplankton in the Tonian Period, evident by comparison with the
502 Mesoproterozoic record (Yan & Liu, 1993; Javaux, Knoll & Walter, 2004; Lamb *et al*. 2009;
503 Agić, Moczydłowska & Yin, 2015a; Sergeev *et al*. 2016), contributed to steady oxygenation
504 of surface waters by the release of free oxygen, increased the production of net organic matter
505 at the base of the food web and supported heterotrophic consumers – all related to the process
506 of photosynthesis. The integrated environmental and evolutionary development with a
507 positive feedback in a sustainable biosphere is first observed in the Tonian Period.
508

509 **CONCLUSIONS**

A Tonian age for the Visingsö Group is well-defined by combining the maximum age of deposition from U-Pb dating of detrital zircons with the minimum age from biochronologic correlation of the Visingsö Group with the Chuar and the lower Mount Harper groups. This restricts its age to ≤886–740 Ma, and furthermore restricts its middle and upper formations to c. 788–740 Ma. These ages can be extrapolated to successions containing similar assemblages in the Caledonides, Greenland, southern Urals, and elsewhere.

We report the presence of diverse assemblage of OWM and several species of VSM, as well as the recovery of mineralized scale microfossils similar to those from the Tonian upper Fifteenmile Group, Yukon, Canada, and for the first time outside Laurentia. We infer the time range of VSM and MSM at c. 788–740 Ma, which is constrained by isotopic datings of strata recording their lowermost and uppermost co-occurrence.

Geochronological constraint on the Visingsö microfossil assemblage is significant for revealing the time sequence of evolutionary events and divergence of auto- and heterotrophic protist lineages and for tracing their passive dispersal and active migration between the palaeocontinents. Presence of cosmopolitan taxa indicates a free connection with global ocean and circulation of surface currents allowing biotic expansion along contiguous continental margins.

The evolution of marine ecosystems comprising similar biotas during the Tonian Period along newly opening marine basins in margins of Baltica (Visingsö, Hedmark, Vadsø, Tanafjord and Barents Sea successions) and Laurentia (Chuar, Uinta Mountain, Pahrump, Little Dal, Mount Harper and Fifteenmile successions), established the first truly global and diverse eukaryotic protistan biosphere.

ACKNOWLEDGEMENTS

Our research was supported by Swedish Research Council (Vetenskåpsrådet) project grants Nr 621-2012-1669 to MM and Nr 621-2014-4375 to VP. Geological Survey of Sweden (SGU) is kindly acknowledged for the access to the Visingsö 1 drillcore. The work of LW was conducted with the kind permission of the SGU Director.

REFERENCES

AGIĆ, H., MOCZYDŁOWSKA, M. & YIN, L-M. 2015a. Affinity, life cycle, and intracellular complexity of organic-walled microfossils from the Mesoproterozoic of Shanxi, China. *Journal of Paleontology* **89**, 28–50.

AGIĆ, H., MOCZYDŁOWSKA, M. & WILLMAN, S. 2015b. Prasinophyte world: biodiversity of organic-walled microfossils from the Cryogenian Visingsö Group, Sweden. 2015 Geological Society of America Annual Meeting, 2015 Baltimore, *Abstracts.*

ALLEN, P. A. & ETIENNE, J. L. 2008. Sedimentary challenge to Snowball Earth. *Nature Geosciences* **1**, 817–825.

ALLISON, C. W. & AWRAMIK, S. M. 1989. Organic-Walled Microfossils from Earliest Cambrian or Latest Proterozoic Tindir Group Rocks, Northwest Canada. *Precambrian Research* **43**, 253–294.

ALLISON, C. W. & HILGERT, J. W. 1986. Scale microfossils from the Early Cambrian of northwest Canada. *Journal of Paleontology* **60**, 973–1015.

ANBAR, A. D. & KNOLL, A. H. 2002. Proterozoic ocean chemistry and evolution: A bioinorganic bridge. *Science* **297**, 1137–1142.

ANBAR, A. D., DUAN, Y., LYONS, T. W., ARNOLD, G. L., KENDALL, B., CREASER, R. A., KAUFMAN, A. J., GORDON, G. W., SCOTT, C., GARVIN, J. & BUICK, R. 2007. A whiff of oxygen before the Great Oxidation Event? *Science* **317**, 1903–1906.

ARNAUD, E., HALVERSON, G.P. & SHIELDS-ZHOU, G. (ed.), 2011. The Geological Record of Neoproterozoic Glaciations. *Geological Society Memoir* **No. 36**, 1–735.

BEKKER, A., HOLLAND, H. D., WANG, P.-L., RUMBLE III, D., STEIN, H. J., HANNAH, J. L., COETZEE, L. L. & BEUKES, N. J. 2004. Dating the rise of atmospheric oxygen. *Nature* **427**, 117–120.

BINGEN, B., BELOUSOVA, E. A. & GRIFFIN, W. L. 2011. Neoproterozoic recycling of the Sveconorwegian orogenic belt: Detrital-zircon data from the Sparagmite basins in the Sveconorwegian Caledonides. *Precambrian Research* **189**, 347–367.

BLOESER, B. 1985. *Melanocyrillium*, A new genus of structurally complex Late Proterozoic microfossils from the Kwagunt Formation (Chuar Group), Grand Canyon, Arizona. *Journal of Paleontology* **59**, 41–765.

BONHOMME, M. G. & WELIN, E. 1983. Rb-Sr and K-Ar isotopic data on shale and siltstone from the Visingsö group, Lake Vättern basin, Sweden. *Geologiska Föreningens i Stockholm Förhandlingar* **105**, 363–366.

BOSAK, T., MACDONALD, F., LAHR, D. & MATYS, E. 2011. Putative Cryogenian ciliates from Mongolia. *Geology* **39**, 1123–1126.

BOSAK, T., LAHR, D. J. G., PRUSS, S. B., MACDONALD, F. A., GOODAY, A. J., DALTON, L. & MATYS, E. 2012. Possible early foraminiferans in post-Sturtian (716–635 Ma) cap carbonates. *Geology* **40,** 67–70.

579 BUTTERFIELD, N. J. 2000. *Bangiomorpha pubescens* n.gen.: implications for the evolution
580 of sex, multicellularity, and the Mesoproterozoic/Neoproterozoic radiation of
581 euakaryotes. *Paleobiology* **26,** 386–404.
582 BUTTERFIELD, N. J. 2009. Oxygen, animals, and oceanic ventilation: an alternative view.
583 *Geobiology*, **7**, 1–7.
584 BUTTERFIELD, N. J. 2011. Animals and the invention of the Phanerozoic Earth system.
585 *Trends Ecological Evolution* **26**, 81–87.
586 CANFIELD, D. E. 1998. A new model for Proterozoic ocean chemistry. *Nature* **396**, 450–
587 453.
588 COHEN, K. M., FINNEY, S. C., GIBBARD, P. L. & FAN, J.-X. 2015. The ICS International
589 Chronostratigraphic Chart, v2015/01.
590 URL:http://www.stratigraphy.org/ICSchart/ChronostratChart2015-01.pdf
591 COHEN, P. A. & KNOLL, A. H. 2012. Scale microfossils from the mid-Neoproterozoic
592 Fifteenmile Group, Yukon Territory. *Journal of Paleontology* **86,** 775–800.
593 COHEN, P. A. & MACDONALD, F. A. 2015. The Proterozoic Record of Eukaryotes.
594 *Paleobiology* **41,** 610–632, doi: 10.1017/pab.2015.25.
595 COHEN, P. A., MACDONALD, F. A., PRUSS, S., MATYS, E. & BOSAK, T., 2015. Fossils
596 of putative marine algae from the Cryogenian göacial interlude of Mongolia. *Palaios*
597 **30,** 238–247.
598 COHEN, P. A., SCHOPF, J. W., BUTTERFIELD, N. J., KUDRYAVTSEV, A. B. &
599 MACDONALD, F. A. 2011. Phosphate biomineralization in mid-Neoproterozoic
600 protists. *Geology*, **39,** 539–542.
601 CONDON, D. J., BOGGIANI, P., FIKE, D., HALVERSON, G. P., KASEMANN, S., KNOLL, A.
602 H., MACDONALD, F. A., PRAVE, A. R. & ZHU, M. 2015. Accelerating
603 Neoproterozoic research through scientific drilling. *Scientific Drilling* **No. 19**, 17–25
604 CORSETTI, F. A. 2015. Life During Neoproterozoic Snowball Earth. *Geology* **43**, 559–560.
605 Doi: 10.1130/focus062015.1.
606 CORSETTI, F. A., AWRAMIK, S. M. & PIERCE, D. 2003. A complex microbiota from
607 Snowball Earth times: Microfossils from the Neoproterozoic Kingston Peak
608 Formation, Death Valley, USA. *Proceedings of the National Academy of Sciences*
609 *USA*, **100,** 4399–4404. Doi: 10.1073/pnas.0730560100.
610 COX, G. M, JARRETT, A., EDWARDS, D., CROCKFORD, P. W., HALVERSON, G.,
611 COLLINS, A. S., POIRIER, A. & LI, Z-X. 2016. Basin redox and primary productivity
612 within the Mesoproterozoic Roper Seaway. *Chemical Geology* 15 pp.
613 doi.org/10.1016/j.chemgeo.2016.06.025.
614 DEHLER, C. M. 2014. Advances in Neoproterozoic biostratigraphy spark new correlations
615 and insight in evolution of life. *Geology* **42**, 731–732. doi: 10.1130/focus0812014.1
616 DEHLER, C. M., ELRICK, M., BLOCH, J. D., CROSSEY, L. J., KARSTROM, K. E. & DES
617 MARAIS D. J. 2005. High-resolution ∂^{13}C stratigraphy of the Chuar Group (ca. 770–
618 742 Ma), Grand Canyon: Implications for mid-Proterozoic climate change. *Geological*
619 *Society of America Bulletin* **117**, 32–45.
620 EYLES, N. & JANUSZCZAK, N. 2007. "Zipper-rift": A tectonic model for Neoproterozoic
621 glaciations during the breakup of Rodinia after 750 Ma. *Earth-Science Reviews* **65,** 1–
622 73.
623 GREY, K. 2005. Ediacaran palynology of Australia. *Association of Australasian*
624 *Palaeontologists Memoir* **31**, 1–439.
625 GREY, K. 2007. The World of the Very Small: Fueling the Animalia. In *The Rise of Animals*
626 *Evolution and Diversification of the Kingdom Animalia* (eds M.A. Fedonkin et al.),
627 pp. 219–231. The Johns Hopkins University Press, Baltimore.
628 HALVERSON, G. P., WADE, B. P., HURTGEN, M. T. & BAROVICH, K. M., 2010.

Neoproterozoic chemostratigraphy. *Precambrian Research* **182**, 337–350.
HOFFMAN, P. F. & SCHRAG, D. P. 2002. The snowball Earth hypothesis: testing the limits of global change. *Terra Nova* **14,** 129–155.
HOLLAND, H. 2002. Volcanic gases, black smokers, and the Great Oxidation Event. *Geochimica et Cosmochimica Acta* **66**, 3811–3826.
HORODYSKI, R. J. 1993. Paleontology of Proterozoic shales and mudstones: Examples from the Belt Supergroup, Chuar Group and Pahrump Group, western USA. *Precambrian Research* **61**, 241–278.
JACKSON, T. A. 2015. Variations in the abundance of photosynthetic oxygen through Precambrian and Paleozoic time in relation to biotic evolution and mass extinctions: evidence from Mn/Fe ratios. *Precambrian Research* **264**, 30–35.
JANKAUSKAS, T. V., MIKHAILOVA, N. S. & GERMAN, T. N. (eds), 1989. Microfossili dokembriya SSSR *(Precambrian microfossils of the USSR).* Trudy Instituta Geologii i Geochronologii Dokembrya SSSR. Akademia Nauk, Leningrad, 188 pp. (in Russian).
JAVAUX, E., KNOLL, A.H. & WALTER, M.R. 2004. TEM evidence for eukaryotic diversity in mid-Proterozoic oceans. *Geobiology* **2**, 121–132.
JOHNSTON, D. T., POULTON, S. W., DEHLER, C., PORTER, S., HUSSON, J., CANFIELD, D. E. & KNOLL, A. H. 2010. An emerging picture of Neoproterozoic ocean chemistry: Insights from the Chuar Group, Grand Canyon, USA. *Earth and Planetary Science Letters* **290**, 64–73.
KAUFMAN, A. J., CORSETTI, F. A. & VARNI, M. A. 2007. The effect of rising atmospheric oxygen on carbon and sulfur isotope anomalies in the Neoproterozoic Johnnie Formation, Dearth Valley, USA. *Chemical Geology* **237,** 47–63.
KNOLL, A. H. 1994. Proterozoic and Early Cambrian protists: Evidence for accelerating evolutionary tempo. *Proceedings of the National Academy of Sciences USA* **91**, 6743–6750.
KNOLL, A. H. 2014. Paleobiological Perspectives on Early Eukaryotic Evolution. In *Cold Spring Harbor Perspectives in Biology* (eds P.J. Keeling & E.V. Koonin), 6, a016121, 1–14.
KNOLL, A. H. & VIDAL, G., 1980. Late Proterozoic vase-shaped microfossils from the Visingsö Beds, Sweden. *Geologiska Föreningen i Stockholm Förhandlingar* **102**, 2017–211.
KNOLL, A. H., JAVAUX, E. J., HEWITT, D. & COHEN, P. 2006. Eukaryotic organisms in Proterozoic oceans. *Philosophical Transactions of the Royal Society London, Series B* **361**, 1023–1038.
LALONDE, S. V. & KONHAUSER, K. O. 2015. Benthic perspective on Earth's oldest evidence for oxygenic photosynthesis. *Proceedings of the National Academy of Sciences USA* **112**, 995–1000.
LAMB, D. M., AWRAMIK, S. M., CHAPMAN, D. J. & ZHU, S. 2009. Evidence for eukaryotic diversifiction in the ~1800 millio-year-old Changzhougou Formation, North China. *Precambrian Research* **173**, 93–104.
LARSEN, M. & NØRGAARD-PEDERSEN, N. 1988. A Sedimentological Analysis of Deltaic Complexes and Alluvial Fan Deposits in the Visingsö Group (Upper Proterozoic), Southern Sweden Vol. l. Institut for Almen Geologi Københavns Universitet, 199 pp.
LENTON, T. M., BOYLE, R. A., POULTON, S. W., SHIELDS-ZHOU, G. A. & BUTTERFIELD, N. J., 2014. Co-evolution of eukaryotes and ocean oxygenation in the Neoproterozoic era. *Nature Geoscience* **7**, 257-265.
LI, Z-X., EVENS, D. A. D. & HALVERSON, G. P. 2013. Neoproterozoic glaciations in a

revised global palaeogeography from the breakup of Rodinia to the assembly of Gondwanaland. *Sedimentary Geology* **294**, 219–232.

LI, C., PLANAVSKY, N. J., LOVE, G. D., REINHARD, C. T., HARDISTY, D., FENG, L., BATES, S. M., HUANG, J., ZHANG, Q, CHU, X. & LYONS, T.W. 2015. Marine redox conditions in the middle Proterozoic ocean and isotopic constraints on authigenic carbonate formation: Insights from the Chuanlinggou Formation, Yanshan Basin, North China. *Geochimica et Cosmochimica Acta,* **150**, 90–105.

LIU, P., XIAO, S., YIN, C., CHEN, S., ZHOU, C. & LI, M. 2014. Ediacaran acanthomorphic acritarchs and other microfossils from chert nodules of the upper Doushantuo Formation in the Yandtze Gorges area, South China. *Paleontology Memoir* 72, 1–139.

LORON, C. 2016. The Biodiversity of Organic-Walled Eukaryotic Microfossils from the Tonian Visingsö Group, Sweden. MSc Thesis, Uppsala University, Department of Earth Sciences, Uppsala, ISSN 1650–6553 Nr **366,** 1–103.

LOVE, G. D., GROSJEAN, E., STALVIES, C., FIKE, D. A., GROTZINGER, J. P., BRADLEY, A. S., KELLY, A. E., BHATIA, M., MEREDITH, W., SNAPE, C. E., BOWRING, S. A., CONDON, D. J. & SUMMONS, R.E. 2009. Fossil steroids record the appearance of Demospongiae during the Cryogenian period. *Nature* **457,** 718–721.

LUNDMARK, A. M. & LAMMINEN, J. 2016. The provenance and setting of the Mesoproterozoic Dala Sandstone, western Sweden, and paleogeographic implications for southwestern Fennoscandia. *Precambrian Research* **275**, 197–208.

LYONS, T. W., REINHARD, C. T. & PLANAVSKY, N. J. 2014. The rise of oxygen in Earth's early ocean and atmosphere. *Nature* **506**, 307–315.

MAGNUSSON, N. H. 1960. Age Determination of Swedish Precambrian Rocks. *Geologisk Föreningens i Stockholm Förhandlingar* **82**, 407–432.

MACDONALD, F. A. & ROOTS, C. F. 2010. Upper Fifteenmile Group in the Ogilvie Mountains and correlations of early Neoproterozoic strata in the northern Cordillera. In *Yukon Exploration and Geology 2009*, (eds K.E. MacFarlane, L.H. Weston & L.R. Blackburn), pp. 237–252, Yukon Geological Survey.

MACDONALD, F. A., COHEN, P. A., DUDÁS, F. Ö. & SCHRAG, D. P. 2010a. Early Neoproterozoic scale microfossils in the Lower Tindir Group of Alaska and the Yukon territory. *Geology* **38**, 143–146.

MACDONALD, F. A., SCHMITZ, M. D., CROWLEY, J. L., ROOTS, C. F., JONES, D. S., MALOOF, A. C., STRAUSS, J. V., COHEN, P. A., JOHNSTON, D.T. & SCHRAG, D. P. 2010b. Calibrating the Cryogenian. *Science* **327**, 1241–1243.

MACDONALD, F. A., SMITH, E. F., STRAUSS, J. V., COX, G. M., HALVERSON, G. P. & ROOTS, C. F. 2011. Neoproterozoic and early Paleozoic correlations in the western Ogilvie Mountains, Yukon. In *Yukon Exploration and Geology 2010* (eds K.E. MacFarlane, L.H. Weston & C. Relf), pp. 161–182. Yukon Geological Survey.

MARTÍ MUS, M. & MOCZYDŁOWSKA, M. 2000. Internal morphology and taphonomic history of the Neoproterozoic vase-shaped microfossils from the Visingsö Group, Sweden. *Norsk Geologisk Tidsskrift* **80**, 213-228.

MILLES, B., WATSON, A. J., GOLDBLATT, C., BOYLE, R. & LENTON, T. M. 2011. Timing of Neoproterozoic glaciations linked to transport-limited global weathering. *Nature Geoscience* **4**, 861–864.

MOCZYDŁOWSKA, M. 2008a. The Ediacaran microbiota and the survival of Snowball Earth conditions. *Precambrian Research* **167**, 1-15.

MOCZYDŁOWSKA, M. 2008b. New records of late Ediacaran microbiota from Poland. *Precambrian Research* **167,** 71-92.

MOCZYDŁOWSKA, M. 2015. Algal affinities of the Ediacaran and Cambrian organic-walled

727 microfossils with internal reproductive bodies: *Tanarium* and other morphotypes.
728 *Palynology* **40,** 83–121. Online 2015, doi.10.1080/01916122.2015.1006341.
729 MOCZYDŁOWSKA, M. & NAGOVITSIN, K. 2012. Ediacaran readiation of organic-walled
730 microbiota recorded in the Ura Formation, Patom Uplift, East Siberia. *Precambrian*
731 *Research* **198–199**, 1–24.
732 MOCZYDŁOWSKA, M., LANDING, E., ZANG, W. & PALACIOS, T. 2011. Proterozoic
733 phytoplankton and timing of Chlorophyte algae origins. *Palaeontology* **54,** 721–733.
734 MORAD, S. & AL-AASM, I. S. 1994. Conditions of formation and diagenetic evolution of
735 Upper Proterozoic phosphate nodules from southern Sweden: evidence from
736 petrology, mineral chemistry and isotopes. *Sedimentary Geology* **88**, 267–282.
737 MUKHERJEE, I. & LARGE, R. R. 2016. Pyrite trace element chemistry of the Velkerri
738 Formation, Roper Group, McArthur Basin: Evidence for atmospheric oxygenation
739 during the Boring Billion. *Precambrian Research* **281,** 13–26.
740 MÖLLER, C., ANDERSSON, J., DYCK, B. & LUNDIN, I. 2015. Exhumation of an eclogite
741 terrane as a hot migmatitic nappe, Sveconorwegian orogeny. *Lithos* **226**, 147–168.
742 NARBONNE, G. M. 2005. The Ediacara biota: Neoproterozoic origin of animals and their
743 Ecosystems. *Annual Reviews of Earth and Planetary Sciences* **33**, 421–442.
744 NARBONNE, G. M., XIAO, S. & SHIELDS, G. A. 2012. The Ediacaran Period. In *The*
745 *Geologic Time Scale 2012* (eds F.M. Gradstein et al.), v. 1, pp. 413–435.
746 NAGY, R. M., PORTER, S. M., DEHLER, C. M. & SHEN, Y. 2009. Biotic turnover driven by
747 eutrophication before the Sturtian low-latitude glaciation. *Nature Geoscience* **2**, 415–
748 418.
749 PARTIN, C. A., BEKKER, A., PLANAVSKY, N. J., SCOTT, C. T., GILL, B. C., LI, C.,
750 PODKOVYROV, V., MASLOV, A., KONHAUSER, K. O., LALONDE, S. V., LOVE, G.
751 D., POULTON, S. W. & LYONS, T. W. 2013. Large-scale fluctuations in Precambrian
752 atmospheric and oceanic oxygen levels from the record of U in shale. *Earth and*
753 *Planetary Sciences Letters* **369–370**, 284–293.
754 PEASE, V., DALY, J. S., ELMING, S.-Å., KUMPULAINEN, R., MOCZYDŁOWSKA, M.,
755 PUCHKOV, V., ROBERTS, D., SAINTOT, A. & STEPHENSON, R. 2008. Baltica in the
756 Cryogenian, 850–630 Ma. *Precambrian Research* **160**, 46–65.
757 PLANAVSKY, N. J., REINHARD, C. T., WANG, X., THOMSON, D., MCGOLDRICK, P.,
758 RAINBIRD, R. H., JOHNSON, T., FISCHER, W. & LYONS, T. W. 2014. Low Mid-
759 Proterozoic atmospheric oxygen levels and the delayed rise of animals. *Science* **346**,
760 635–638.
761 PLANAVSKY, N. J., TARHAN, L. G., BELLEFROID, E. J., EVANS, D. A. D.,
762 REINHARD, C. T., LOVE, G. D. & LYONS, T. W. 2015. Late Proterozoic transitions
763 in climate, oxygen, and tectonics, and the rise of complex life. In: Earth-Life
764 Transitions: Paleobiology in the Context of Earth System Evolution. *The*
765 *Paleontological Society Papers* **21**, 1–36.
766 PORTER, S. M. 2006. The Proterozoic fossil record of heterotrophic eukaryotes. In
767 *Neoproterozoic Geobiology and Paleobiology* (eds S.Xiao & A.J. Kaufman), **27**, 1–
768 21, Elsevier.
769 PORTER, S. M. & KNOLL, A. H. 2000. Testate amoebae in the the Neoproterozoic Era:
770 evidence from vase-shaped microfossils in Chuar Group, Grand Canyon. *Paleobiolog,*
771 **26,** 360–385.
772 PORTER, S. M. & RIEDMAN, L. A. 2016. Systematics of organic-walled microfossils from
773 the ca. 780–740 Ma Chuar Group, Grand Canyon, Arizona. *Journal of Paleontology*
774 **90**, 815–853.
775 PORTER, S. M., MEINSTERFELD, R. & KNOLL, A. H. 2003. Vase-shaped microfossils from

776 the Neoproterozoic Chuar Group, Grand Canyon: A classification guided by modern
777 testate amoebae. *Journal of Paleontology*, **77**, 409–429.
778 POULTON, S. W. & CANFIELD, D. E. 2011. Ferruginous conditions: a dominant feture of the
779 ocean through Earth's history. *Elements* **7**, 107–112.
780 RIEDMAN, A. L., PORTER, S. M., HALVERSON, G. P., HURTGEN, M. T. & JUNIUM, C. K.
781 2014. Organic-walled microfossil assemblage from glacial and interglacial
782 Neoproterozoic units of Australia and Svalbard. *Geology* **42**, 1011–1014.
783 SAHOO, S. K., PLANAVSKY, N. J., JIANG, G., KENDALL, B., OWENS, J. D., WANG, X.,
784 SHI, X., ANBAR, A. D. & LYONS, T. W. 2016. Oceanic oxygenation events in the
785 Ediacaran ocean. *Geobiology* **14,** 457–468.
786 SCHIRRMEISTER, B. E., GUGGER, M. & DONOGHUE, P. C. J. 2015. Cyanobacteria and the
787 Great Oxidation Event: evidence from genes and fossils. *Palaeontology* **58,** 769–785.
788 SCHOPF, J. W. 1992. Proterozoic Prokaryotes: Affinities, Geologic Distribution, and
789 Evolutionary Trends. In *The Proterozoic Biosphere A Multidisciplinary Study* (eds
790 J.W. Schopf & C. Klein), pp. 195–218, Cambridge University Press.
791
792 SERGEEV, V. N. 2006. Precambrian Microfossils on Cherts: their Paleobioogy, Classification
793 and Biostratigraphic Usefulness. *Moscow, GEOS, Transactions of the Geological*
794 *Institute*, **567**, 1–280. (In Russian).
795 SERGEEV, V. N., KNOLL, A. H. & GROTZINGER, J. P. 1995. Paleobiology of the
796 Mesoproterozoic Billyakh Group, Anabar Uplift, northeastern Siberia. *Paleontological*
797 *Society Memoir* **39**, 1–37.
798 SERGEEV, V. N., KNOLL, A. H., VOROBEVA, N. G. & SERGEEVA, N. D. 2016.
799 Microfossils from the lower Mesoproterozoic Kaltasy Formation, East European
800 Platform. *Precambrian Research* **278,** 87–107.
801 SPENCE, G. H., LE HERON, D. L. & FAIRCHILD, I. J. 2016. Sedimentological perspectives
802 on climatic, atmospheric and environmental chenge in the Neoproterozic Era.
803 *Sedimentology* **63**, 253–306.
804 STEPHENS, M. B., RIPA, M., LUNDSTRÖM, I., PERSSON, L., BERGMAN, T., AHL, M.,
805 WAHLGREN, C. H., PERSSON, P. O. & WICKSTRÖM, L. 2009. Synthesis of the
806 bedrock geology in the Bergslagen region. Fennoscandian Shield, South-central
807 Sweden. *Sveriges geologiska undersökning (SGU) report* Ba **58**, 1–259.
808 SPERLING, E. A., FRIEDER, C. A., RAMAN, A. V., GIRGUIS, P. R., LEVIN, L. A. &
809 KNOLL, A. H. 2013. Oxygen, ecology, and the Cambrian radiation of animals.
810 *Proceedings of the National Academy of Sciences USA* **110**, 13446–13451.
811 STRAUSS, J. V., ROONEY, A. D., MACDONALD, F. A., BRANDON, A. D. & KNOLL, A. H.
812 2014. 740 Ma vase-shaped microfossils from Yukon, Canada: Implications for
813 Neoproterozoic chronology and biostratigraphy. *Geology* **42**, 659–662.
814 SWANSON-HYSELL, N. L., MALOOF, A. C., CONDON, D. J., JENKIN, G. R. T., ALENE,
815 M., TREMBLAY, M. M., TESEMA, T., ROONEY, A. D. & HAILEAB, B. 2015.
816 Stratigraphy and geochronology of the Tambien Group, Ethiopia: Evidence for
817 globally synchronous carbon isotope change in the Neoproterozoic. *Geology* **43**, 323–
818 326.
819 SÖDERLUND, U., ISACHSEN, C., BYLUND, G., HEAMAN, L. M., PATCHETT, P. J.,
820 VERVOORT, J. & ANDERSSON, U. B. 2005. U-Pb baddeleyite ages and Hf, Nd
821 isotope chemistry constraining repeated mafic magmatism in the Fennoscandian
822 Shield from 1.6 to 0.9 Ga. *Contributions to Mineralogy and Petrology*, **150**, 174-194.
823 TANG, D., SHI, X., WANG, X. & JIANG, G. 2016. Extremaly low oxygen concentration in
824 mid-Proterozoic shallow seawaters. *Precambrian Research* **276,** 145–157.
825 TANG, Q., PANG, K., YUAN, X., WAN, B. & XIAO, S. 2015. Organic-walled microfossils

826 from the Tonian Gouhou Formation, Huaibei region, North China Craton, and their
827 biostratigraphic implications. *Precambrian Research* **266**, 296–318.
828 TANG, Q., PANG, K., XIAO, S., YUAN, X., OU, Z. & WAN, B. 2013. Organic-walled
829 microfossils from the early Neoproterozoic Liulaobei Formation in the Huinan region
830 of North china and their biostratigraphic significance. *Precambrian Research* **236**,
831 157–181.
832 TURNER, E. C. & BEKKER, A. 2016. Thick sulfate evaporate accumulations marking a mid-
833 Neoproterozoic oxygenation event (Ten Stone Formation, Northwest Territories,
834 Canada). *Geological Society of America Bulletin* **128**, 203–222.
835 ULMIUS, J., ANDERSSON, J. & MÖLLER, C. 2015. Hallandian 1.45 Ga high-temperature
836 metamorphism in Baltica: P–T evolution and SIMS U–Pb zircon ages of aluminous
837 gneisses, SW Sweden. *Precambrian Research* **265**, 10-39.
838 VAN KRANENDONK, M. J., ALTERMANN, W., BEARD, B. L., HOFFMSAN, P. F.,
839 JOHNSON, C. M., KASTING, J. F., MELEZHIK, V. A., NUYMAN, A. P., PAPINEAU,
840 D. & PIRAJNO, F. 2012. A Chronostratigraphic Division of the Precambrian. In *The*
841 *Geologic Time Scale 2012* (eds F.M. Gradstein et al.), v. 1, pp. 299–392.
842 VIDAL, G. 1972. Algal stromatolites from the Late Precambrian of Sweden. *Lethaia* **5**,
843 353–368.
844 VIDA, G. 1974. Late Precambrian microfossils from the basal sandstone unit of the Visingsö
845 beds, South Sweden. *Geologica et Palaeontologica* **8**, 1–14.
846 VIDAL, G. 1976. Late Precambrian microfossils from the Visingsö Beds in southern Sweden.
847 *Fossils and Strata* **9**, 1–57.
848 VIDAL, G. 1979. Acritarchs from the Upper Proterozoic and Lower Cambrian of East
849 Greenland. *Grønlands Geologiske Undersøgelse Bulletin* **134**, p. 1–40.
850 VIDAL, G. 1982. Den prepaleozoiska sedimentära berggrunden. In: Description to the map of
851 solid rocks Hjo NO. *Sveriges geologiska undersökning, Serie Af* **120**, 52–76.
852 VIDAL, G. 1985. Prepaleozoisk sedimentberggrund. In Persson, L., Brunn, Å. & Vidal, G.,
853 Beskrivning till bergrundskartan Hju SO (Description to the map of solid rocks Hju
854 SO), *Sveriges Geologiska Undersökning Serie Af* **134,** 77–91.
855 VIDAL, G. 1994. Early ecosystems: Limitations imposed by the fossil record. In *Early Life on*
856 *Earth* (ed. S. Bengtson, S.), pp. 298–311, Nobel Symposium No. 84, Columbia
857 University Press, New York.
858 VIDAL, G. & FORD, T. 1985. Microbiotas from the late Proterozoic Chuar Group (northern
859 Arizona) and Uinta Mountain Group (Utah) and their chronostratigraphic implications.
860 *Precambrian Research* **28**, 349–489.
861 VIDAL, G. & MOCZYDŁOWSKA, M. 1995. The Neoproterozoic of Baltica–stratigraphy,
862 palaeobiology and general geologic evolution. *Precambrian Research* **73**, 197–216.
863 VIDAL, G. & MOCZYDŁOWSKA-VIDAL, M. 1997. Biodiversity, speciation, and extinction
864 trends of Proterozoic and Cambrin phytoplankton. *Paleobiology* **23**, 230–246.
865 VIOLA, G., HENDERSON, I. H. C., BINGEN, B. & HENDRIKS, B. W. H. 2011. The
866 Grenvillian–Sveconorwegian orogeny in Fennoscandia: Back-thrusting and
867 extensional shearing along the "Mylonite Zone". *Precambrian Research* **189**, 368-
868 388.
869 XIAO, S., ZHOU, C., LIU, P., WANG, D. & YUAN, X. 2014a. Phosphatized acanthomorphic
870 acritarchs and related microfossils from the Ediacaran Doushantuo Formation at
871 Weng'an (South China) and their implications for biostratigraphic correlation. *Journal*
872 *of Paleontology* **88**, 1–67.
873 XIAO, S., SHEN, B., TANG, Q., KAUFMAN, A. J., YUAN, X., LI, J. & QIAN, M. 2014b.
874 Biostratigraphic and chemostratigraphic contraints on the age of early Neoproterozoic
875 carbonate successions in North China. *Precambrian Research* **246**, 208–225.

YAN, Y. & LIU, Z. 1993. Significance of eukaryotic organisms in the microfossil flora of Changcheng System. *Acta Micropalaeontologica Sinica* **10**, 167–180.

YE, Q., TONG, J., XIAO, S., ZHU, S., AN, Z., TIAN, L. AND HU, J. 2015. The survival of benthic macroscopic phototrophs on a Neoproterozoic snowball earth. *Geology* **43**, 507–510.

ZHANG, W., ROBERTS, D. & PEASE, V. 2015a. Provenance characteristics and regional implications of Neoproterozoic, Timanian-margin successions and a basal Caledonian nappe in northern Norway. *Precambrian Research*, **268**, 153–167.

ZHANG, W., ROBERTS, D. & PEASE, V. 2015b. Provenance of sandstones from Caledonian nappes in Finnmark, Norway: Implications for Neoproterozoic–Cambrian palaeogeography. *Tectonophysics*, http://dx.doi.org/10.1016/j.tecto.2015.09.001.

ZHANG, S., WANG, X., WANG, H., BJERRUM, C. J., HAMMARLUND, E. U., COSTA, M. M., CONNELLY, J. N., ZHANG, B., SU., J. & CANFIELD, D. E. 2016. Sufficient oxygen for animal respiration 1,4000 million years ago. *Proceedings of the National Academy of Sciences USA* **113**, 1731–1736.

FIGURE CAPTIONS

Figure 1. (a) Map of Baltoscandia showing tectonostratigraphic domains of the Caledonides and the Fennoscandian Shield basement with the distribution of the remnant Proterozoic sediments. (b) Extension of the Visingsö Group along Lake Vättern. (c) Lithologic succession with position of studied samples and distribution of microfossils. Modified from Vidal, 1982; Lundmark and Lamminen, 2016. Abbreviations: SF - Sveconorwegian deformation front, MZ - Mylonite Zone, OWM- organic-walled microfossils, VSM - vase-shaped microfossils, SM - scale microfossils, S - stromatolites, fm. – formation.

Figure 2. New record of vase-shaped microfossils (b, c) and newly-discovered mineralized scale microfossils (a, b, d) preserved in phosphatic nodules in the upper formation of the Visingsö Group. (a) *Paleomegasquama arctoa*, Slide 6, K-35-2. (b) *Cycliocyrillium torquata* (specimen on left side), and *Bicorniculum brochum* (specimen on right side), Slide 6, V40-3. (c) *Melanocyrillium hexadiadema* (upper specimen), Slide 7, M10-4. (d) *Archeoxybaplan polykeramoides*, Slide 7, J24-2. Scale bar equals to 15 μm in a, 30 μm in b, 50 μm in c, 20 μm in d. Collection PMU-V72G14, Slides 6–7. England Finder Coordinates provided for each specimen.

910

911 Figure 3. New record of organic-walled microfossils from the upper formation of the Visingsö
912 Group, (a-i) light transmitted and (j-k) scanning electron micrographs (j-k). (a)
913 *Squamosphaera colonialica,* V14-66-4-(J44). (b) *Synsphaeridium* sp., V14-14-3-(F30-3). (c)
914 *Simia* sp., V14-14-3-(J28). (d) *Simia annulare*, V14-14-3-(P24-4). (e) *Pterospermopsimorpha*
915 *pileiformis*, V14-79-4-(M37-4). (f) *Leiosphaeridia ternata*, V14-14-3-(L25-3). (g)
916 *Leiosphaeridia* sp., V14-36-5-(S44). (h-i) *Lanulatisphaera laufeldii*, V14-66-4-(C40-3); V14-
917 66-4-(U39-1). (j-k) *Cerebrosphaera globosa* (Ogurtsova and Sergeev, 1989) Sergeev and
918 Schopf, 2010; j, V14-80-4-L57; k, V14-52-1-04. Scale bars equal 20 μm for light transmitted
919 micrographs. Collection PMU-Visingsö.2014 (V14- followed by the sample and slide
920 numbers, and England Finder Coordinates).

921

922 Figure 4. Probability density distribution plots of detrital zircons and their ages from the
923 Visingsö Group sandstones in stratigraphic order. The Sveconorwegian (0.90–1.14 Ga),
924 Hallandian (1.38–1.47 Ga), Gothian (1.52-1.66 Ga), and TIB (1.66–1.86 Ga) sources are
925 indicated (grey bars).

926

927

928

929

930

931

932

933

934

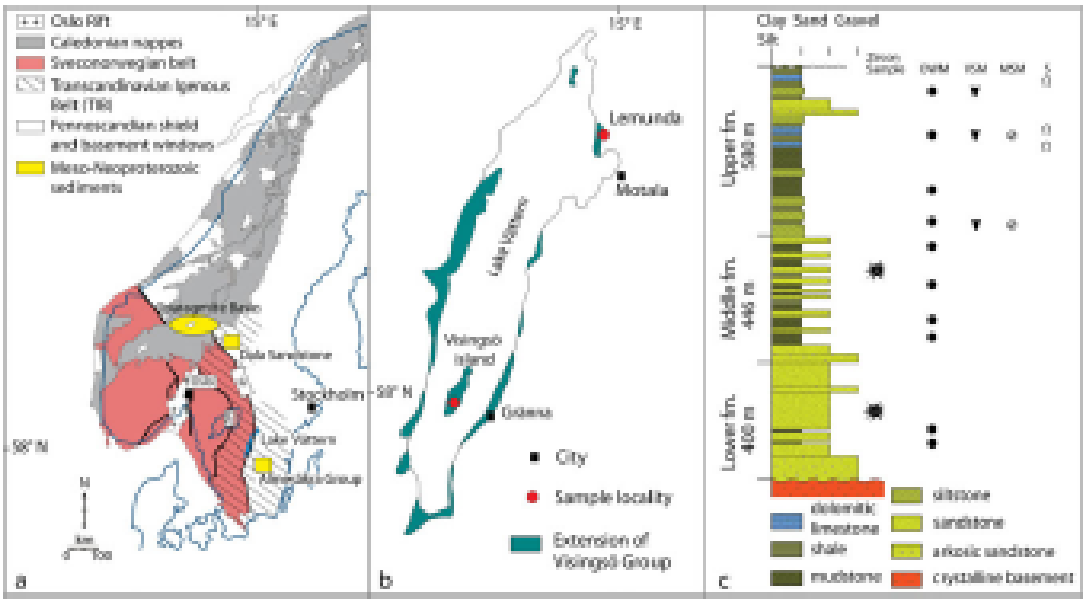

Figure 1. (a) Map of Baltoscandia showing tectonostratigraphic domains of the Caledonides and the Fennoscandian Shield basement with the distribution of the remnant Proterozoic sediments. (b) Extension of the Visingsö Group along Lake Vättern. (c) Lithologic succession with position of studied samples and distribution of microfossils. Modified from Vidal (1982) and Lundmark & Lamminen (2016). Abbreviations: SF – Sveconorwegian deformation front; MZ – Mylonite Zone; OWM – organic-walled microfossils; VSM – vase-shaped microfossils; MSM – mineralized scale microfossils; S – stromatolites; fm. – formation.

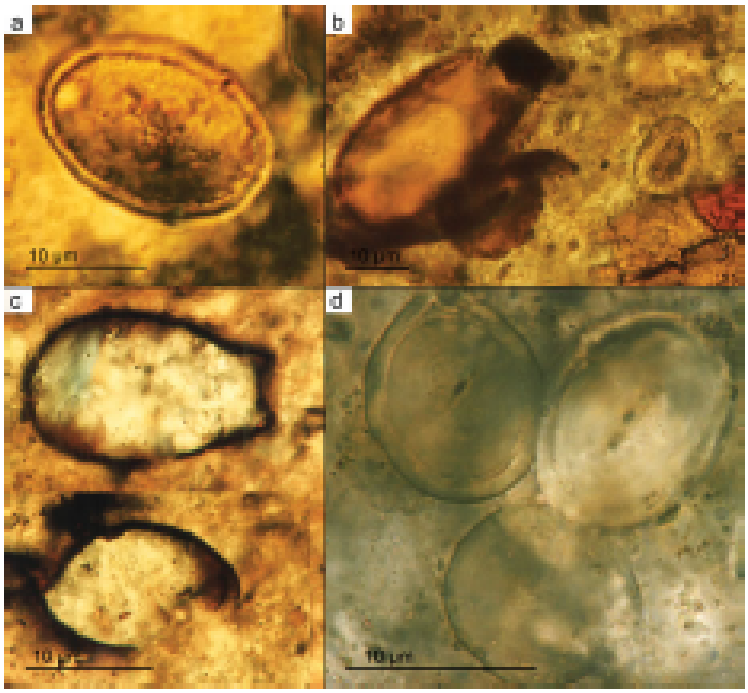

Figure 2. New record of vase-shaped microfossils (b, c) and newly discovered mineralized scale microfossils (a, b, d) preserved in phosphatic nodules in the upper formation of the Visingsö Group. (a) *Paleomorganquasma arctica*, Slide 6, K-35-2. (b) *Cyclocyrillium torquata* (specimen on left side), and *Ilicovesiculum brochum* (specimen on right side), Slide 6, V40-3. (c) *Melanocyrillium hexadiadema* (upper specimen), Slide 7, M10-4. (d) *Archecorybephon polyhexonoides*, Slide 7, J24-2. Scale bar equal to 15 µm in (a), 30 µm in (b), 50 µm in (c), 20 µm in (d). Collection PMU-VT2014, Slides 6–7. England Finder Coordinates provided for each specimen.

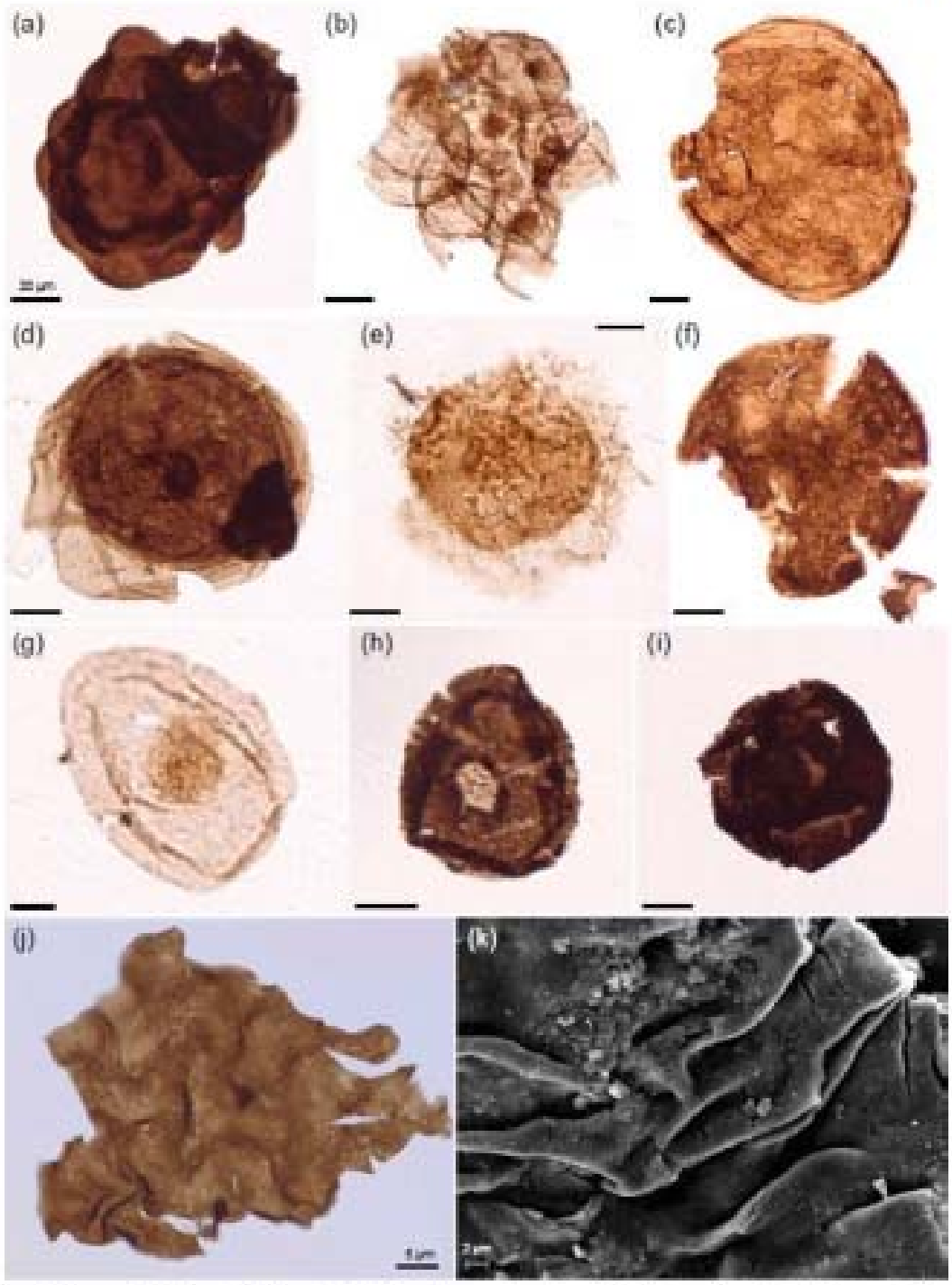

Figure 3. New record of organic-walled microfossils from the upper formation of the Visingsö Group. (a–i) light transmitted and (j, k) scanning electron micrographs. (a) *Squamosphaera colonialica*, V14-66-4-(J44). (b) *Synsphaeridium* sp., V14-14-3-(F10-3). (c) *Valeria lophostriata*, V14-14-3-(J28). (d) *Simia annulare*, V14-14-3-(P24-4). (e) *Pterosperma protomorphe pileiformis*, V14-79-4-(M37-4). (f) *Leiosphaeridia tenuissima*, V14-14-3-(L25-3). (g) *Leiosphaeridia* sp., V14-36-3-(S44). (h, i) *Lamalisiphaera laufeldi*, V14-66-4-(C40-3); V14-66-4-(U39-1). (j, k) *Cerebrosphaera globosa* (Ogurtsova & Sergeev, 1989) Sergeev & Schopf, 2010. (j) V14-80-4-157; (k) V14-52-1-04. Scale bars equal 20 μm for light transmitted micrographs. Collection PMU-Visingsö.2014 (V14- followed by the sample and slide numbers, and England Finder Coordinates).

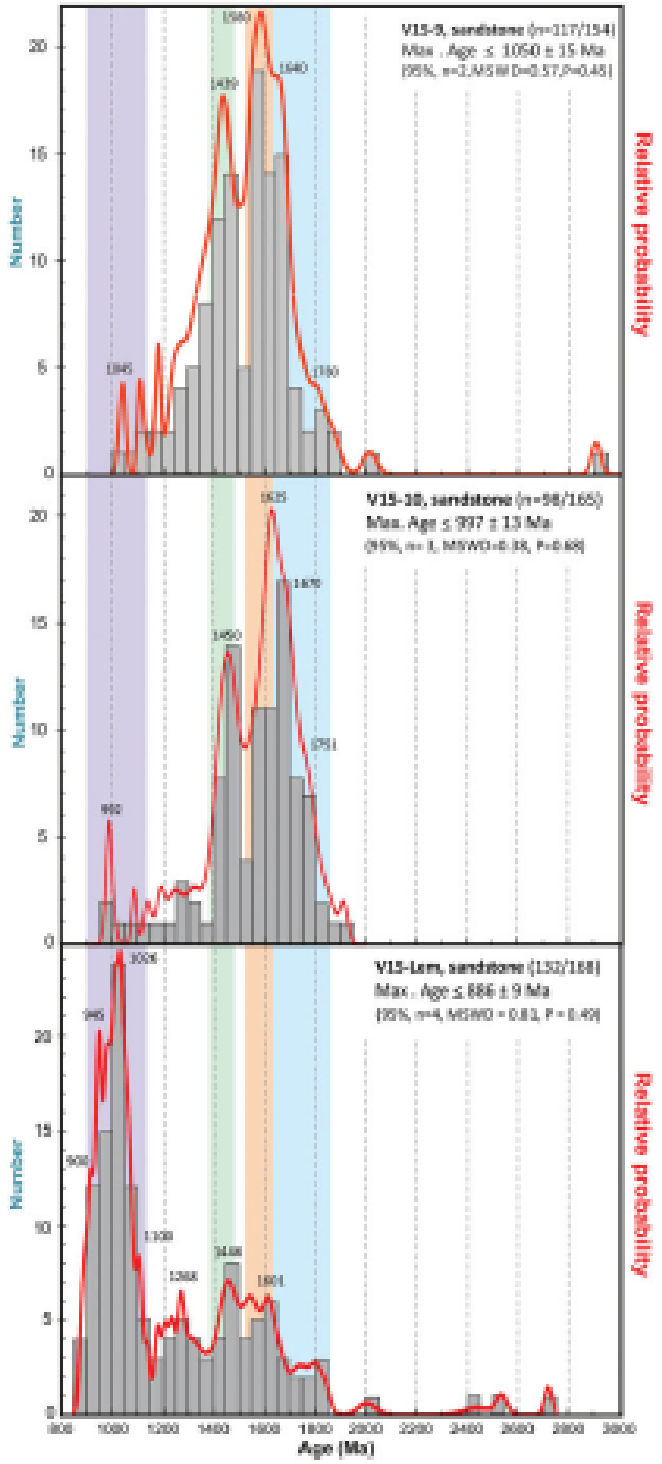

Figure 4. Probability density distribution plots of detrital zircons and their ages from the Visingsö Group sandstones in stratigraphic order. The Sveconorwegian (0.90–1.14 Ga), Hallandian (1.38–1.47 Ga), Gothian (1.52-1.66 Ga) and TIB (1.66–1.86 Ga) sources are indicated (grey bars).